

RESEARCH LETTER

10.1029/2018GL077042

Key Points:

- Agulhas Current has an impact on South African rainfall along the eastern coast
- The mechanism for low-level convergence and collocated rainfall show similarities to that for the Gulf Stream
- Regional atmospheric model experiments indicate that the Agulhas Current generates convective rainfall along the coast

Supporting Information:

- Supporting Information S1

Correspondence to:

A. S. Nkwinkwa Njouodo,
 a.nkwinkwa@yahoo.fr

Citation:

Nkwinkwa Njouodo, A. S., Koseki, S., Keenlyside, N., & Rouault, M. (2018). Atmospheric signature of the Agulhas Current. *Geophysical Research Letters*, *45*, 5185–5193. <https://doi.org/10.1029/2018GL077042>

Received 5 JAN 2018

Accepted 13 APR 2018

Accepted article online 19 APR 2018

Published online 29 MAY 2018

Atmospheric Signature of the Agulhas Current

Arielle Stela Nkwinkwa Njouodo^{1,2} , Shunya Koseki³ , Noel Keenlyside^{3,4} ,
 and Mathieu Rouault^{1,2} 

¹Department of Oceanography, MARE Institute, University of Cape Town, Cape Town, South Africa, ²Nansen-Tutu Centre for Marine Environmental Research, University of Cape Town, Cape Town, South Africa, ³Geophysical Institute, Bjerknes Centre for Climate Research, University of Bergen, Bergen, Norway, ⁴Nansen Environmental and Remote Sensing Center, Bjerknes Centre for Climate Research, Bergen, Norway

Abstract Western boundary currents play an important role in the climate system by transporting heat poleward and releasing it to the atmosphere. While their influence on extratropical storms and oceanic rainfall is becoming appreciated, their coastal influence is less known. Using satellite and climate reanalysis data sets and a regional atmospheric model, we show that the Agulhas Current is a driver of the observed band of rainfall along the southeastern African coast and above the Agulhas Current. The Agulhas current's warm core is associated with sharp gradients in sea surface temperature and sea level pressure, a convergence of low-level winds, and a co-located band of precipitation. Correlations among wind convergence, sea level pressure, and sea surface temperature indicate that these features show high degree of similarity to those in the Gulf Stream region. Model experiments further indicate that the Agulhas Current mostly impacts convective rainfall.

Plain Language Summary We demonstrate that the Agulhas Current has an impact on rainfall of the eastern coast of South Africa and above it. We manage to simulate that effect. This will lead to improve the weather, climate prediction, and climate services for this region. We present the convincing evidence that the Agulhas Current influences the atmosphere, and we show that the underlying mechanisms may be similar to those found for Gulf Stream. Our study is made possible by the combined use of high-resolution climate observations, climate reanalysis, and numerical modeling. Oceanographers, climatologists, and meteorologists have now a deeper understanding of an important driver of the climate and weather of South Africa. Future climate change projections of South Africa rainfall will need to integrate this effect of the Agulhas Current.

1. Introduction

The Agulhas Current is the strongest southern hemisphere western boundary current, transporting around 70 Sverdrup (Sv, 1Sv = 10⁶ m³ s⁻¹; Beal & Bryden, 1999) of warm Indian Ocean water along the southeast coast of Africa. As for the Gulf Stream and the Kuroshio, the Agulhas Current is warmer than the surrounding ocean, and this leads to high turbulent sensible and latent heat fluxes (Rouault et al., 2003) when colder and drier air is advected above the current. However, only a few studies have investigated the impact of the Agulhas Current on local weather and climate. Radiosondes and heat flux measurements above the Agulhas Current show that the vigorous exchange of moisture and energy above the current penetrates into the troposphere to at least 1,500 m (Lee-Thorp et al., 1999; Rouault et al., 2000). This phenomenon causes distinct cloud lines above the Agulhas Current during fair weather high-pressure synoptic conditions (Lutjeharms et al., 1986; Rouault et al., 2000). Moreover, moisture produced by the Agulhas Current can be advected inland (Jury et al., 1997; Lee-Thorp et al., 1999; Rouault et al., 2000). In particular, rain rate and the diurnal cycle of rainfall along the eastern coast of South Africa are related to the proximity of the Agulhas Current (Jury et al., 1993; Rouault et al., 2013). Furthermore, moisture advected from the Current was hypothetically linked to an extreme weather system (Rouault et al., 2002). Jury (2015) found a relationship between El Niño–Southern Oscillation, Southern Africa Interior rainfall, and sea surface temperature (SST) in a large domain encompassing the Agulhas Current system as a whole. These climatic impacts of Agulhas Current may even have played an important role in the survival of *Homo sapiens* in Africa in the distant past (Marean et al., 2007).

Regional impacts of the Agulhas Current on Southern African climate have not been thoroughly investigated using numerical models, although the climatic impact of the greater Agulhas Current system was studied using a coarse resolution model (Reason, 2001). Similarly, first-generation climate reanalysis was too coarse to properly study the climatic impacts of the current (Rouault et al., 2003; Rouault & Lutjeharms, 2003)

because they did not resolve its core where the turbulent sensible and latent heat fluxes are 5 times stronger than the surrounding water. Recent studies indicate that a model horizontal resolution of at least 0.25° is required to resolve ocean-atmosphere interaction over such currents (Parfitt et al., 2016; Smirnov et al., 2015). Several mechanisms explaining the role of the Gulf Stream and the Kuroshio on precipitation are proposed (Minobe et al., 2008, 2010; O'Neill et al., 2017; Parfitt & Czaja, 2016; Vanni re et al., 2017; Xu et al., 2011; Sasaki et al., 2012). However, the influence of the Agulhas Current on the weather and climate of Southern Africa is not well known compared to the impact of the Gulf Stream and the Kuroshio on weather and climate. The aim of this study is to investigate using observations, reanalysis, and numerical model experiments how the warm SST associated with the Agulhas Current affects the low-level atmosphere and rainfall.

2. Data and Methods

2.1. Data and Atmospheric Model

We use various parameters of the Climate Forecast System Reanalysis (CFSR, Saha et al., 2010) provided by the National Centers for Environmental Prediction from 2001 to 2005. These 5 years are enough to evaluate the climatic impact offshore South Africa of the core of the Agulhas Current, which has little interannual variations and few perturbations in its track (Krug & Tournadre, 2012; Rouault & Penven, 2011). We use the 0.05° by 0.05° climatology (1998–2007) of Tropical Rainfall Measuring Mission precipitation radar (TRMM PR, Biasutti et al., 2012) for precipitation, the 0.25° by 0.25° resolution GlobCurrent (2002–2005) surface geostrophic current derived from altimetry (Johannessen et al., 2015; Rio et al., 2014), the 0.25° by 0.25° resolution (2001–2005) advanced very high resolution radiometer-based optimal interpolation SST (Reynolds et al., 2007), and the 0.25° by 0.25° resolution (1999–2007) Scatterometer Climatology of Ocean Winds (Risien & Chelton, 2008) for the validation of CFSR 10-m wind speed (Table S1 in the supporting information). All the climatologies are computed from at least 5 years of data, with the period from 2002 to 2005 overlapping.

The Weather Research and Forecast/Advanced Research (Skamarock & Klemp, 2008) system version 3.7.1 is applied to investigate the impact of the core of the Agulhas Current on the atmosphere. The model domain is 17°S – 43°S and 8°E – 52°E (Figure S2 in the supporting information), and the resolution is 25×25 km, with 56 vertical eta-coordinate levels. We perform two experiments: a control (CTL) driven with interannually varying, high-resolution, observed SST and a sensitivity experiment (smoothed SST, SMTH) driven with SST smoothed to remove the sharp SST gradients associated with the Agulhas Current (Figure S2), and that is otherwise identical to CTL. Both experiments cover the period 2001 to 2005, with lower boundary condition taken from advanced very high resolution radiometer (Reynolds et al., 2007), and lateral boundary conditions taken from ERA-Interim reanalysis (Dee et al., 2011; Simmons et al., 2007). Further details on the model experiments can be found in the supporting information.

2.2. Method: Diagnostic Analysis of Pressure Adjustment Mechanism

We use a simple Marine Atmospheric Boundary Layer model (MABL) to investigate the relationship between the near surface wind convergence and sea level pressure (SLP) Laplacian (Lindzen & Nigam, 1987; Minobe et al., 2008): $\varepsilon u - fv = -p_x/\rho_0$, $\varepsilon v + fu = -p_y/\rho_0$, where x and y are the zonal and meridional coordinates; u and v are the zonal and meridional surface wind (frictional stresses from above the MABL are neglected); ρ_0 and p are the density and pressure in the MABL; ε denotes the constant damping coefficient; and f represents the Coriolis parameter. Surface wind convergence is linked to the SLP Laplacian by a linear relationship, $-\rho_0(u_x + v_y) = (p_{xx} + p_{yy})\varepsilon/(\varepsilon^2 + f^2)$. SLP and underlying SST are also related (Lindzen & Nigam, 1987) according to $\varepsilon p + H(u_x + v_y) = -\gamma T$, where T is the SST, γ is a constant, and H is the equivalent depth of the MABL. Thus, a linear relationship between surface pressure and SST may indicate an impact of the ocean on the atmosphere. Here we compare the Laplacian of these two quantities to isolate the strength of this relation at the finer scale of the Agulhas warm core. Recent studies have questioned the relevance of this diagnostic model (section 4), but it still serves for comparison to previous studies of northern hemisphere western boundary currents.

3. Results

3.1. High-Resolution Observations Over the Agulhas Current

We analyze the annual climatological mean state using satellite observations and modern atmospheric reanalysis to reveal a clear relationship between the Agulhas Current and precipitation (Figure 1). The Agulhas

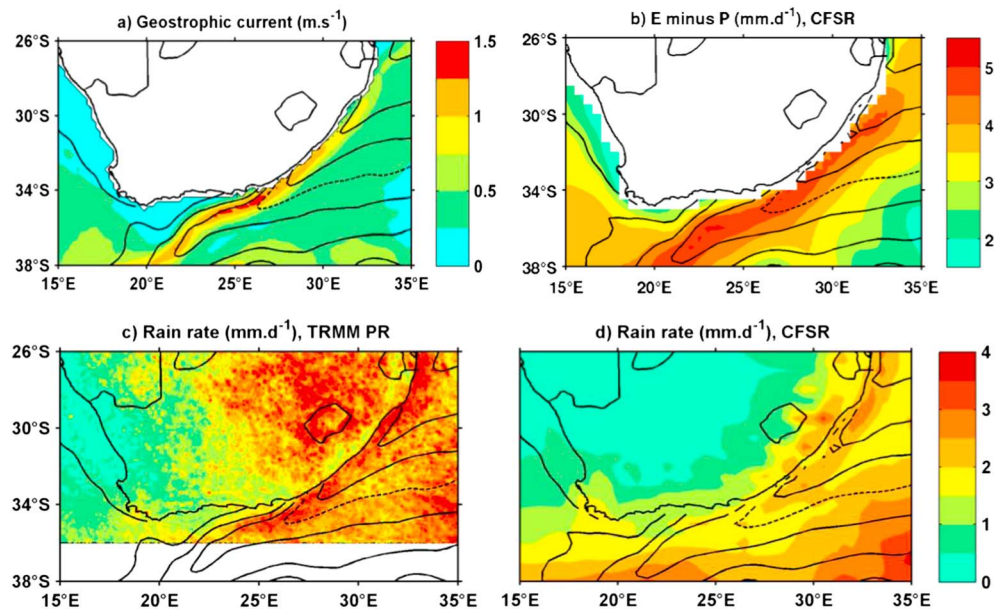


Figure 1. Annual climatology: (a) surface geostrophic current from GlobCurrent at 0 m depth, (b) Climate Forecast System Reanalysis (CFSR) evaporation minus precipitation and rain rate of (c) Tropical Rainfall Measuring Mission Precipitation Radar, and (d) CFSR. The solid contours represent annual climatology of optimal interpolation sea surface temperature (SST) and CFSR SST, respectively, for (a) and (c) and (b) and (d) with 1° interval; the dash line is 22° C SST.

Current is 80–100 km wide and runs south-westward along the eastern coast of South Africa, following roughly the continental shelf until it retroflects and flows westward (Figure 1a). Here we focus on the core of the current, which is a few degrees warmer than the surrounding ocean (contours Figure 1), and on the region where the current hugs the coast. The SST varies from 27°C off the East Coast of South Africa to 23°C in the retroflexion in late summer, and from 22°C to 18°C in late winter (not shown). The turbulent latent heat flux (turbulent flux of moisture) above the sharp tongue of SST is high, reaching values of up to 220 W/m^2 annually. The high flux is caused by the advection of oceanic colder and drier air over the current, together with the destabilizing effect of the SST gradient on the surface MABL and the wind speed (Lee-Thorp et al., 1999; Rouault et al., 2000).

The annual mean rainfall rate from the TRMM PR (Biasutti et al., 2012) derived observations and the CFSR reanalysis (Saha et al., 2010) both show a narrow band of precipitation along the eastern coast of South Africa, just over the core of the Agulhas Current (Figures 1c and 1d). TRMM PR-derived rainfall frequency shows an equally striking relation (Figure S1a). In the Agulhas region, annual mean precipitation varies from 3 to 4 mm/d for TRMM PR, while a few degrees to the east, it is about 1 mm/d less. CFSR captures the rainband, especially near the coast to the east, although it differs from TRMM PR by 1 to 2 mm/d (and by more over the interior of the continent, which is not our domain of research).

3.2. Mechanisms for Rainfall Over the Agulhas Current

The CFSR reanalysis shows that local evaporation exceeds rainfall by between 2 to 5 mm/d over the entire region, with the greatest excess over the Agulhas Current (Figure 1b). Thus, local moisture supply is consistent with the broad scale rainfall over the region, as well as the enhanced rainfall over the Agulhas Current. However, moisture alone does not lead to rainfall; air masses must be lifted to saturation by low-level wind convergence, atmospheric convective processes, or by frontal processes. Frontal processes are likely responsible for the broad scale rainfall occurring south of our region of interest; here sharp SST gradients anchor the storm track of extratropical cyclones (Nakamura et al., 2004) and thereby frontal rainfall (Hand et al., 2014; Parfitt et al., 2016). This mechanism may explain rainfall patterns over the Agulhas Return Current, where the current and the southern hemisphere storm track align (Hoskins & Hodges, 2005).

Sharp SST gradients can also impact surface winds and thereby generate lower-level atmospheric convergence and vertical motion, which can penetrate deep into the free troposphere (Chelton & Xie, 2010).

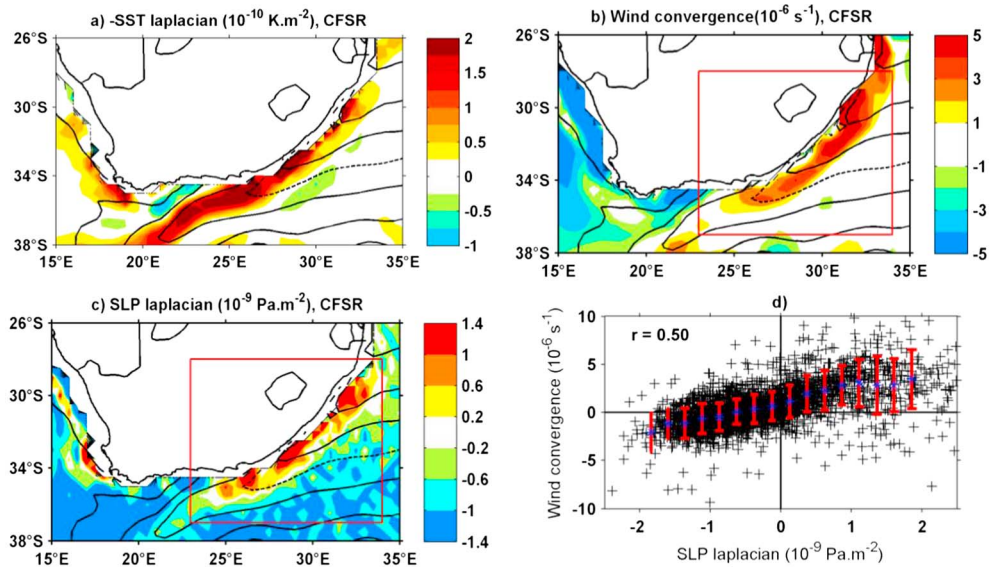


Figure 2. Climate Forecast System Reanalysis annual climatology of (a) sign reversed sea surface temperature (SST) Laplacian, (b) wind convergence (positives values), and (c) sea level pressure (SLP) Laplacian. Annual mean SST is contoured as in Figure 1. (d) Scatter plot showing the relation between wind convergence and SLP Laplacian based on monthly climatology within the region 28–37°E, 23–34°S indicated by the red boxes in (b) and (c). The blue stars represent the mean values for each interval; the error bars in red are ± 1 standard deviation of wind convergence for each bin of SLP Laplacian.

Vertical mixing is one mechanism for the wind response to SST fronts (Wallace et al., 1989): Above warm SST, the lower atmosphere becomes unstable due to large turbulent heat fluxes. This mechanism is observed in regions with strong SST gradients (Xie, 2004), including the Agulhas Return Current (O’neill et al., 2005). Another dynamical explanation for the wind response to SST is the pressure adjustment mechanism (Back & Bretherton, 2009; Lindzen & Nigam, 1987): SST modifies the MABL temperature so that the resultant pressure anomalies induce surface wind convergence over warm SST and wind divergence over cold SST. Earlier studies implicated the pressure adjustment mechanism in producing the observed pattern of wind convergence and divergence over major SST frontal regions (Minobe et al., 2008; Shimada & Minobe, 2011). Recent studies suggest that the low-level convergence and associated rainband over the Gulf Stream is instead the result of the interaction of synoptic-scale atmospheric variability with the sharp SST front (O’Neill et al., 2017; Parfitt et al., 2016; Sheldon et al., 2017).

To assess whether the increase of rainfall over the core of the Agulhas Current may result from similar mechanisms to those for the Gulf Stream, we compare the annual climatology of SST Laplacian, wind convergence, and SLP Laplacian. According to the pressure adjustment mechanism, a tight relation among these quantities indicates that warmer (colder) SST drives lower (higher) SLP, and in turn enhances surface wind convergence (divergence; Minobe et al., 2008; section 2). The Laplacian acts as a spatial high-pass filter that highlights sharp gradient. The negative SST Laplacian (Figure 2a) exhibits a distinct structure along the eastern coast of South Africa, collocated with the rainband. (The SST Laplacian is reversed in sign for the convenience of comparing results.) The satellite-derived SST Laplacian (Figure S1b) is similar to the CFSR one, but stronger in amplitude because of the data’s higher resolution. Along the eastern coast of South Africa, a predominant narrow band of 10-m wind convergence is collocated with the rainfall and negative SST Laplacian (Figure 2b). CFSR reproduces quite well the band of wind convergence found in the higher resolution satellite-based Scatterometer Climatology of Ocean Winds climatology (see Figure S1c). Convergence and divergence are also present in the retroflection region around 38.5°S, 22°E and downstream along the meandering Agulhas Return Current (Shimada & Minobe, 2011; not shown). The SLP Laplacian shows a positive band along the eastern coast of South Africa (Figure 2c) that is also collocated with the SST Laplacian, wind convergence, and rainfall. This indicates that SLP above the Agulhas Current is linked to the underlying SST and may be consistent with the pressure adjustment mechanism (Lindzen & Nigam, 1987; Minobe et al., 2008).

We quantify the relationship among the terms of the pressure adjustment mechanism for the maritime region over the Agulhas Current (28–37°S, 23–34°E; red boxes in Figures 2b and 2c). The relationship between SLP Laplacian and surface wind convergence exhibits a spatial correlation coefficient of 0.50, statistically significant at the 95% level (Figure 2d). The scatterplot shows that the relation between SLP Laplacian and surface wind convergence is approximately linear (Figure 2d). However, there is greater scatter among positive values of SLP Laplacian and wind convergence, as compared to negative values. The negative SST Laplacian and SLP Laplacian exhibit a stronger spatial correlation of 0.71, significant at the 95% level (Figure S1d). These significant relations are consistent with those found over the Gulf Stream, indicating that the low-level convergence could be the result of the interaction of synoptic-scale atmospheric variability with the sharp SST front and may drive rainfall over the Agulhas Current.

3.3. Agulhas Current Impact in Regional Atmospheric Model Experiments

We perform two regional model experiments (Skamarock & Klemp, 2008) to isolate the role of the Agulhas warm core on the atmosphere (section 2). The regional model experiment with observed SST (CTL) reproduces the rainband along the Agulhas Current realistically (Figure 3a). In CTL, the Agulhas Current precipitation rate varies between 2 and 4 mm/d (Figure 3a) and is similar to the TRMM PR observations (Figure 1c) but is up to 2 mm/d more than CFSR (Figure 1d). Over land the simulated annual precipitation is stronger than in the observations and reanalysis. This may be due to a strong sensitivity of the cumulus convection schemes to the topography, a common issue with this regional model (Pohl et al., 2014).

The rainband along the South Africa coast adjacent to the Agulhas Current is strongly reduced in the experiment with SMTH compared to CTL (Figure 3b). The difference is up to 1.4 mm/d with a maximum offshore Kwazulu-Natal (around 30.5°S; 31.5°E). The coastal rainfall in SMTH is around 40% less than in CTL (Figure S3a). The coastal rainband is mostly due to convective precipitation: rainfall due to large-scale circulation is almost identical between the two simulations (Figures S3b and S3c), while the coastal convective precipitation is highly diminished in SMTH (Figures S3d and S3e). Thus, the experiments show that the warmer Agulhas Current SST enhances precipitation along the eastern coast of South Africa.

The wind convergence and the positive SLP Laplacian over the Agulhas Current are relatively well simulated compared to satellite estimates and reanalyzed output (Figures 3c and 3e). (Note that the simulated SLP Laplacian is influenced by inland values along the ocean grid adjacent to land probably due to orography.) The difference of wind convergence between CTL and SMTH shows a well-defined maximum over the Agulhas Current (Figure 3d) that is collocated with the corresponding difference of SLP Laplacian (Figure 3f). The magnitude of the difference in wind convergence is about half of the magnitude of CTL, while the differences in SLP are of similar magnitude to that of CTL. The spatial correlation between the SLP Laplacian and wind convergence computed from the difference of the experiments is 0.55 (Figure 3g), which is similar to the value from CFSR reanalysis ($r = 0.50$). The spatial correlation between SLP Laplacian and the negative SST Laplacian computed from the difference of the experiments is 0.70 (Figure 3h), which is also similar to that from CFSR reanalysis ($r = 0.71$). These results provide strong support that SST gradients anchor the rainband over the Agulhas.

3.4. Vertical Atmospheric Structure Over the Agulhas

The CFSR reanalysis shows strong upward motion in the lower troposphere between 950 and 850 hPa that is collocated with the rainband over the core of the Agulhas Current (Figure 4a). Above, there is a distinct structure of the wind divergence between 850 and 700 hPa, and by 650 hPa, the upward motion is much reduced and there is mostly large-scale convergence (Figures 4d and S4a and S4d). The signature of the Agulhas Current is hardly found at 650 hPa. At lower levels there are corresponding narrow bands of subsidence either side of the upward motion that contribute to a local lower tropospheric overturning circulation. Thus, reanalysis suggests that convection reaches only the lower troposphere in accord with measurements done above the Agulhas Current (Lee-Thorp et al., 1999; Rouault et al., 2000). The regional model experiments show that the Agulhas Current drives this local overturning circulation. In CTL, the vertical motion at lower levels is weaker and occurs closer to the coast than in the reanalysis, and there is a broader band of subsidence to the east of the upward motion (Figure 4b). Consistent with the weaker upward motion, the horizontal divergence above is weaker and there are hardly any indications of upward motion at 650 hPa (Figures 4e and S4b and S4e). The difference between CTL and SMTH confirms that SST associated with the Agulhas Current

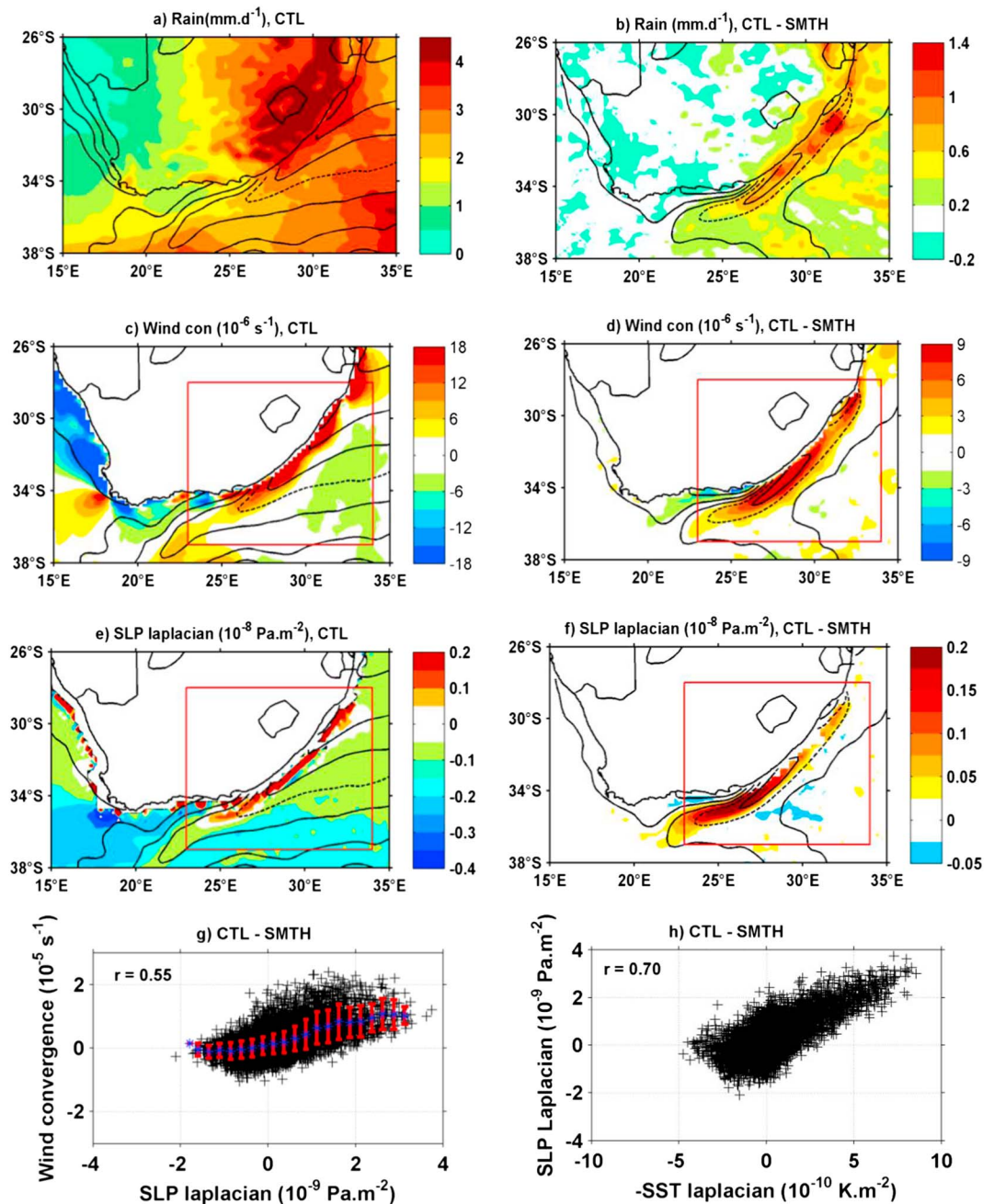


Figure 3. The annual mean (a) rainfall, (c) wind convergence, and (e) SLP Laplacian simulated by control (CTL) are plotted as in Figure 2 with the sea surface temperature (SST) contours of CTL overlaid. (b, d, and f) The impact of smoothing the SST gradients in the Agulhas Current region on these quantities is shown by the differences between CTL and smoothed SST (SMTH); the contours show the SST difference between CTL and SMTH (0.5 °C interval and dashed line for 1 °C). Shown also are the relations (g) between wind convergence and SLP Laplacian and (h) between SLP Laplacian and sing inverted SST Laplacian for monthly climatology differences CTL and SMTH within the region 28–37°E, 23–34°S.

drives this vertical circulation, which is associated with the rainband along the southern African coast (Figures 4c and 4f and S4c and S4f).

4. Discussion and Implication for Climate Modeling and Prediction

We have shown using high-resolution satellite-derived estimates, climate reanalysis, and regional atmospheric model experiments that the warm core of the Agulhas Current drives a band of precipitation along

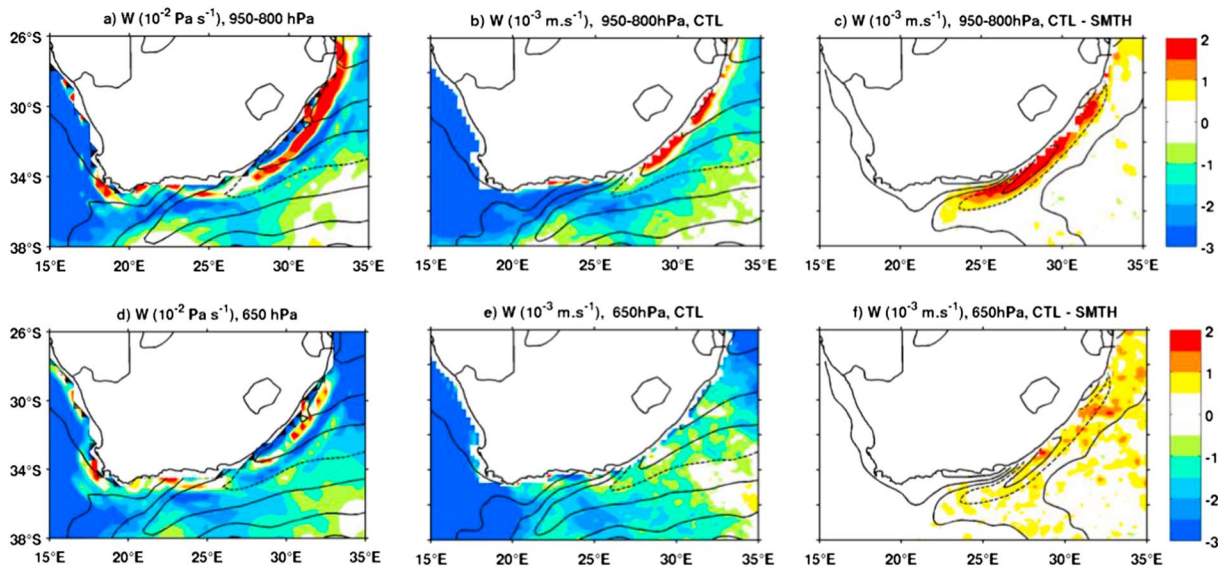


Figure 4. The annual mean of vertical velocity vertically averaged between 950 and 800 hPa (a) Climate Forecast System Reanalysis, (b) control (CTL), and (c) the difference between CTL and smoothed SST. (d, e, and f) Their respective 650-hPa vertical velocity is represented with the SST contours overlaid.

the coast and offshore South Africa. Our results indicate that the sharp SST gradients are responsible for the formation of the rainband and drive a local narrow overturning circulation in the lower troposphere. We found that spatially smoothing the SST leads to a decrease of 50% for wind convergence, of 100% for SLP Laplacian, and a 40% reduction in precipitation over the core of the Agulhas Current.

Diagnosis of the pressure adjustment mechanism identifies a very similar relation to that for the Gulf Stream (Minobe et al., 2008). Recent studies, however, indicate that the anchoring of precipitation over the Gulf Stream front is mainly associated with the atmospheric frontal precipitation associated with synoptic scale extratropical cyclones (O'Neill et al., 2017; Parfitt et al., 2016; Sheldon et al., 2017; Vannière et al., 2017). A similar mechanism might act over the Agulhas Current, as a large part of the rainfall there is also related to atmospheric fronts (Catto et al., 2012).

Our simulations indicate that the Agulhas current impacts terrestrial rainfall the most in austral summer and the least in winter (Figure S5). The positive anomalies of vertical motion (Figure S6) along the inland coast in summer (DJF) are collocated with the increased in rainfall when CTL is compared to SMTH. The diurnal cycle is an important driver for terrestrial rainfall in summer there (Pohl et al., 2014; Rouault et al., 2013), and low-level convergence associated with the orography could also be a factor in enhancing summer rainfall. A complete understanding of how the Agulhas Current drives terrestrial precipitation in this region will therefore involve in depth analysis of both the diurnal cycle and seasonality of various parameters.

Our atmospheric model simulations indicate that up to 20% of the coastal precipitation is related to the warm core of the Agulhas Current. This may represent a lower limit as increasing the model's resolution might increase the strength of ocean-atmosphere interaction (Smirnov et al., 2015). Thus, it is important to resolve the fine structure of ocean temperature for simulating the climate of the region. This has implications for the prediction of South African weather and climate and for understanding past and present climate.

References

- Back, L. E., & Bretherton, C. S. (2009). On the relationship between SST gradients, boundary layer winds, and convergence over the tropical oceans. *Journal of Climate*, 22(15), 4182–4196. <https://doi.org/10.1175/2009JCLI2392.1>
- Beal, L. M., & Bryden, H. L. (1999). The velocity and vorticity structure of the Agulhas Current at 32 S. *Journal of Geophysical Research*, 104(C3), 5151–5176. <https://doi.org/10.1029/1998JC900056>
- Biasutti, M., Yuter, S. E., Burleyson, C. D., & Sobel, A. H. (2012). Very high resolution rainfall patterns measured by TRMM precipitation radar: Seasonal and diurnal cycles. *Climate Dynamics*, 39(1–2), 239–258. <https://doi.org/10.1007/s00382-011-1146-6>
- Catto, J. L., Jakob, C., Berry, G., & Nicholls, N. (2012). Relating global precipitation to atmospheric fronts. *Geophysical Research Letters*, 39(10), L10805. <https://doi.org/10.1029/2012GL051736>

Acknowledgments

This work has been performed with the support of the SCAMPI project (234205/H30) funded by the Research Council of Norway under the SANCOOP program. The authors thank B. C. Bhatt in University of Bergen, B. Pohl in University of Burgundy, and R. Fonseca in Luelá University of Technology for helping to set up and perform WRF simulations. Computing resources were provided by NoTur (nn9039k and ns9039k). NK is supported by the ERC (grant 648982), and the work was also supported by the NFR (grant 233680/E10). Thanks to ESA funding under GlobCurrent DUE project AO/1-7472/13/I-LG; GlobCurrent products are available for free. Thanks to Robert Dattore from the DATA SUPPORT SECTION of the National Center for Atmospheric Research (NCAR/UCAR) for his help with CFSR reanalysis. The authors thank the NRF SARCHI chair of Ocean Land Atmosphere modeling, ACCESS, NRF, DST, DAAD-AIMS South Africa, and the Nansen Tutu Center for their support. The data on which this study is based are publicly available at the following links: <http://kage.ideo.columbia.edu:81/SOURCES/LDEO/ClimateGroup/DATASETS>, <http://cioss.coas.oregonstate.edu/scow/>, <https://rda.ucar.edu/>, <https://www.ncdc.noaa.gov/oisst/>, and <http://www.globcurrent.org>.

- Chelton, D. B., & Xie, S. P. (2010). Coupled ocean-atmosphere interaction at oceanic mesoscales. *Oceanography*, 23(4), 52–69. <https://doi.org/10.5670/oceanog.2010.05>
- Dee, D. P., Uppala, S. M., Simmons, A. J., Berrisford, P., Poli, P., Kobayashi, S., et al. (2011). The ERA-Interim reanalysis: configuration and performance of the data assimilation system. *Quarterly Journal of the Royal Meteorological Society*, 137, 553–597. <https://doi.org/10.1002/qj.828>
- Hand, R., Keenlyside, N., Omrani, N. E., & Latif, M. (2014). Simulated response to inter-annual SST variations in the Gulf Stream region. *Climate Dynamics*, 42(3–4), 715–731. <https://doi.org/10.1007/s00382-013-1715-y>
- Hoskins, B. J., & Hodges, K. I. (2005). A new perspective on Southern Hemisphere storm tracks. *Journal of Climate*, 18(20), 4108–4129. <https://doi.org/10.1175/JCLI3570.1>
- Johannessen, J. A., Chapron, B., Collard, F., Rio, M. H., Piollé, J. F., Quartly, G. D., et al. (2015). Globcurrent: Sentinel-3 synergy in action. In *Proceedings of Sentinel-3 for Science Workshop (2–5 June 2015, Venice, Italy)*, ESA, Special Publication (Vol. 734, p. 2). <http://adsabs.harvard.edu/abs/2015ESASP.734.2J>
- Jury, M., Rouault, M., Weeks, S., & Shormann, M. (1997). Atmospheric boundary layer fluxes and structure across a transition zone in south-eastern Africa. *Boundary-Layer Meteorology*, 83(2), 311–330. <https://doi.org/10.1023/A:1000295700599>
- Jury, M. R. (2015). Passive suppression of South African rainfall by the Agulhas Current. *Earth Interactions*, 19, 1–14. <https://doi.org/10.1175/EI-D-15-0017.1>
- Jury, M. R., Valentine, H. R., & Lutjeharms, J. R. (1993). Influence of the Agulhas Current on summer rainfall along the southeast coast of South Africa. *Journal of Applied Meteorology*, 32(7), 1282–1287. [https://doi.org/10.1175/1520-0450\(1993\)032%3C1282:IOTACO%3E2.0.CO;2](https://doi.org/10.1175/1520-0450(1993)032%3C1282:IOTACO%3E2.0.CO;2)
- Krug, M., & Tournadre, J. (2012). Satellite observations of an annual cycle in the Agulhas Current. *Geophysical Research Letters*, 39, L15607. <https://doi.org/10.1029/2012GL052335>
- Lee-Thorp, A. M., Rouault, M., & Lutjeharms, J. R. E. (1999). Moisture uptake in the boundary layer above the Agulhas Current: A case study. *Journal of Geophysical Research*, 104(C1), 1423–1430. <https://doi.org/10.1029/98JC02375>
- Lindzen, R. S., & Nigam, S. (1987). On the role of sea surface temperature gradients in forcing low-level winds and convergence in the tropics. *Journal of the Atmospheric Sciences*, 44(17), 2418–2436. [https://doi.org/10.1175/1520-0469\(1987\)044%3C2418:OTROSS%3E2.0.CO;2](https://doi.org/10.1175/1520-0469(1987)044%3C2418:OTROSS%3E2.0.CO;2)
- Lutjeharms, J. R. E., Mey, R. D., & Hunter, I. T. (1986). Cloud lines over the Agulhas Current. *South African Journal of Science*, 82(11), 635–640.
- Marean, C. W., Bar-Matthews, M., Bernatchez, J., Fisher, E., Goldberg, P., Herries, A. I., et al. (2007). Early human use of marine resources and pigment in South Africa during the Middle Pleistocene. *Nature*, 449(7164), 905–908. <https://doi.org/10.1038/nature06204>
- Minobe, S., Kuwano-Yoshida, A., Komori, N., Xie, S. P., & Small, R. J. (2008). Influence of the Gulf Stream on the troposphere. *Nature*, 452(7184), 206–209. <https://doi.org/10.1038/nature06690>
- Minobe, S., Miyashita, M., Kuwano-Yoshida, A., Tokinaga, H., & Xie, S. P. (2010). Atmospheric response to the Gulf Stream: Seasonal variations. *Journal of Climate*, 23(13), 3699–3719. <https://doi.org/10.1175/2010JCLI3359.1>
- Nakamura, H., Sampe, T., Tanimoto, Y., & Shimpo, A. (2004). Observed associations among storm tracks, jet streams and midlatitude oceanic fronts. *Earth's Climate*, 329–345.
- O'Neill, L. W., Chelton, D. B., Esbensen, S. K., & Wentz, F. J. (2005). High-resolution satellite measurements of the atmospheric boundary layer response to SST variations along the Agulhas Return Current. *Journal of Climate*, 18(14), 2706–2723. <https://doi.org/10.1175/JCLI3415.1>
- O'Neill, L. W., Haack, T., Chelton, D. B., & Skillingstad, E. (2017). The Gulf Stream Convergence Zone in the time-mean winds. *Journal of the Atmospheric Sciences*, 74(7), 2383–2412.
- Parfitt, R., & Czaja, A. (2016). On the contribution of synoptic transients to the mean atmospheric state in the Gulf Stream region. *Quarterly Journal of the Royal Meteorological Society*, 142(696), 1554–1561. <https://doi.org/10.1002/qj.2689>
- Parfitt, R., Czaja, A., Minobe, S., & Kuwano-Yoshida, A. (2016). The atmospheric frontal response to SST perturbations in the Gulf Stream region. *Geophysical Research Letters*, 43(5), 2299–2306.
- Pohl, B., Rouault, M., & Roy, S. S. (2014). Simulation of the annual and diurnal cycles of rainfall over South Africa by a regional climate model. *Climate Dynamics*, 43(7–8), 2207–2226. <https://doi.org/10.1007/s00382-013-2046-8>
- Reason, C. J. C. (2001). Evidence for the influence of the Agulhas Current on regional atmospheric circulation patterns. *Journal of Climate*, 14(12), 2769–2778. [https://doi.org/10.1175/1520-0442\(2001\)014%3C2769:EFTIOT%3E2.0.CO;2](https://doi.org/10.1175/1520-0442(2001)014%3C2769:EFTIOT%3E2.0.CO;2)
- Reynolds, R. W., Smith, T. M., Liu, C., Chelton, D. B., Casey, K. S., & Schlax, M. G. (2007). Daily high-resolution-blended analyses for sea surface temperature. *Journal of Climate*, 20(22), 5473–5496. <https://doi.org/10.1175/2007JCLI1824.1>
- Rio, M. H., Mulet, S., & Picot, N. (2014). Beyond GOCE for the ocean circulation estimate: Synergetic use of altimetry, gravimetry, and in situ data provides new insight into geostrophic and Ekman currents. *Geophysical Research Letters*, 41, 8918–8925. <https://doi.org/10.1002/2014GL061773>
- Risien, C. M., & Chelton, D. B. (2008). A global climatology of surface wind and wind stress fields from eight years of QuikSCAT scatterometer data. *Journal of Physical Oceanography*, 38(11), 2379–2413. <https://doi.org/10.1175/2008JPO3881.1>
- Rouault, M., Lee-Thorp, A. M., & Lutjeharms, J. R. E. (2000). The atmospheric boundary layer above the Agulhas Current during alongcurrent winds. *Journal of Physical Oceanography*, 30(1), 40–50. [https://doi.org/10.1175/1520-0485\(2000\)030%3C0040:TABLAT%3E2.0.CO;2](https://doi.org/10.1175/1520-0485(2000)030%3C0040:TABLAT%3E2.0.CO;2)
- Rouault, M., & Lutjeharms, J. R. E. (2003). Microwave satellite remote sensing of SST around Southern Africa. *South African Journal of Science*, 99, 489–494.
- Rouault, M., Reason, C. J. C., Lutjeharms, J. R. E., & Beljaars, A. C. M. (2003). Underestimation of latent and sensible heat fluxes above the Agulhas Current in NCEP and ECMWF analyses. *Journal of Climate*, 16(4), 776–782. [https://doi.org/10.1175/1520-0442\(2003\)016%3C0776:UOLASH%3E2.0.CO;2](https://doi.org/10.1175/1520-0442(2003)016%3C0776:UOLASH%3E2.0.CO;2)
- Rouault, M., Roy, S. S., & Balling, R. C. (2013). The diurnal cycle of rainfall in South Africa in the austral summer. *International Journal of Climatology*, 33(3), 770–777. <https://doi.org/10.1002/joc.3451>
- Rouault, M., White, S. A., Reason, C. J. C., Lutjeharms, J. R. E., & Jobard, I. (2002). Ocean–atmosphere interaction in the Agulhas Current region and a South African extreme weather event. *Weather and Forecasting*, 17(4), 655–669. [https://doi.org/10.1175/1520-0434\(2002\)017%3C0655:OAIITA%3E2.0.CO;2](https://doi.org/10.1175/1520-0434(2002)017%3C0655:OAIITA%3E2.0.CO;2)
- Rouault, M. J., & Penven, P. (2011). New perspectives on Natal pulses from satellite observations. *Journal of Geophysical Research*, 116, C07013. <https://doi.org/10.1029/2010JC006866>
- Saha, S., Moorthi, S., Pan, H. L., Wu, X., Wang, J., Nadiga, S., et al. (2010). The NCEP Climate Forecast System Reanalysis. *Bulletin of the American Meteorological Society*, 91(8), 1015–1058. <https://doi.org/10.1175/2010BAMS3001.1>
- Sasaki, Y. N., Minobe, S., Asai, T., & Inatsu, M. (2012). Influence of the Kuroshio in the East China Sea on the early summer (baisu) rain. *Journal of Climate*, 25(19), 6627–6645. <https://doi.org/10.1175/JCLI-D-11-00727.1>
- Sheldon, L., Czaja, A., Vannière, B., Morcrette, C., Sohet, B., Casado, M., & Smith, D. (2017). A ‘warm path’ for Gulf Stream-troposphere interactions. *Tellus A: Dynamic Meteorology and Oceanography*, 69(1), 1299397. <https://doi.org/10.1080/16000870.2017.1299397>

- Shimada, T., & Minobe, S. (2011). Global analysis of the pressure adjustment mechanism over sea surface temperature fronts using AIRS/Aqua data. *Geophysical Research Letters*, *38*, L06704. <https://doi.org/10.1029/2010GL046625>
- Simmons, A., Uppala, S., Dee, D., & Kobayashi, S. (2007). ERA-Interim: New ECMWF reanalysis products from 1989 onwards. *ECMWF Newsletter*, *110*, 25–35.
- Skamarock, W. C., & Klemp, J. B. (2008). A time-split nonhydrostatic atmospheric model for Weather Research and Forecasting applications. *Journal of Computational Physics*, *227*(7), 3465–3485. <https://doi.org/10.1016/j.jcp.2007.01.037>
- Smirnov, D., Newman, M., Alexander, M. A., Kwon, Y. O., & Frankignoul, C. (2015). Investigating the local atmospheric response to a realistic shift in the Oyashio sea surface temperature front. *Journal of Climate*, *28*(3), 1126–1147. <https://doi/abs/10.1175/JCLI-D-14-00285.1>
- Vannière, B., Czaja, A., Dacre, H., & Woollings, T. (2017). A “cold path” for the Gulf Stream-troposphere connection. *Journal of Climate*, *30*(4), 1363–1379. <https://doi.org/10.1175/JCLI-D-15-0749.1>
- Wallace, J. M., Mitchell, T. P., & Deser, C. (1989). The influence of sea-surface temperature on surface wind in the eastern equatorial Pacific: Seasonal and interannual variability. *Journal of Climate*, *2*(12), 1492–1499. [https://doi.org/10.1175/1520-0442\(1989\)002%3C1492:TIOSST%3E2.0.CO;2](https://doi.org/10.1175/1520-0442(1989)002%3C1492:TIOSST%3E2.0.CO;2)
- Xie, S. P. (2004). Satellite observations of cool ocean-atmosphere interaction. *Bulletin of the American Meteorological Society*, *85*(2), 195–208. <https://doi.org/10.1175/BAMS-85-2-195>
- Xu, H., Xu, M., Xie, S.-P., & Wang, Y. (2011). Deep atmospheric response to the spring Kuroshio Current over the East China Sea. *Journal of Climate*, *24*(18), 4959–4972. <https://doi.org/10.1175/JCLI-D-10-05034.1>